04

Volume transmission holograms in lithium niobate crystals with surface copper doping for photovoltaic tweezers

© R.I. Anisimov, A.S. Temereva, A.A. Kolmakov, S.M. Shandarov

Tomsk State University of Control Systems and Radioelectronics, Tomsk, Russia

e-mail: roman.anisimov.00@mail.ru

Received August 07, 2023
Revised August 07, 2023
Accepted September 28, 2023

The results of experimental studies, theoretical analysis and numerical simulations of the features of the volume transmission holograms' formation by the interference pattern of laser beams with high contrast in the X-cut $LiNbO_3:Cu$, fabricated by diffusion from a metal film, are presented. Analytic formulas that take the inhomogeneities of the distribution of copper ions and the absorption index of recording beams over the thickness of the sample into account are derived to describe the time evolution of the amplitude of the first spatial harmonic of the field. The material parameters of the $LiNbO_3:Cu$ structure are estimated. A comparative analysis of the spatial distribution of the amplitude of the first harmonic of the photorefractive hologram's field in two types of $LiNbO_3:Cu$ structures is performed. We concluded that it is necessary to use X-cut $LiNbO_3:Cu$ diffusion structures characterized by similar distributions of impurity centers, which maximums are localized near the boundary used to capture micro- and nanoparticles, for the implementation of photovoltaic tweezers.

Keywords: photorefractive grating, diffraction efficiency, angular selectivity, lithium niobate.

DOI: 10.61011/EOS.2023.10.57759.5480-23

Introduction

One of the approaches to the implementation of optically controlled manipulators of micro- and nano-objects includes using strong evanescent electric fields appearing above a surface the crystals of lithium niobate under heterogeneous illumination thereof [1–6]. Substrates for the optical tweezers of this type are implemented by crystals of lithium niobate, which are doped with iron [1–5] or copper [6], wherein the impurity ions provide a high photovoltaic response. The advantages of the photovoltaic tweezers include multiple usage of single-crystal substrates and minimizing overheating of captured items due to application of low-power radiation sources [5].

The paper [6] has demonstrated aggregation of the dielectric nanoparticles by the evanescent electric fields of the photorefractive gratings on a surface of the sample $LiNbO_3:Cu$, which is fabricated by diffusion doping of the X-cut congruent lithium niobate from a copper metal film. Copper can be diffused into the lithium niobate samples at the temperatures of 600°C [7], 800°C [8] and 1000°C [6,9–11], from the metal films Cu [6,9–11] and the powder oxide CuO [7,8].

The photovoltaic tweezers shall be implemented based on the diffusion $LiNbO_3:Cu$ plates with the important characteristics, which include sample-depth distributions of the impurity centers C_{Cu^+} and $C_{Cu^{2+}}$ in the charge states Cu^+ and Cu^{2+}, respectively [12]. It should be noted that the data of [6–11] about the nature of these distributions are contradictory. It follows from the results of [9] that in the sample of the thickness of 1 mm the concentration Cu^+ decreases only by 20% with increase in the distance from the X-surface with the copper metal film deposited thereon. However, in [6] the distribution of the absorption coefficient $k_{523}(x)$ at the wavelength of 532 nm is obtained as the Gaussian function with the half-width of $\Delta x = 316\,\mu$m and a maximum at the X-boundary, which was used for diffusion out of the Cu metal film therethrough. For this sample $LiNbO_3:Cu$, when analyzing formation of the dynamic photorefractive gratings in [12], it was assumed that the distributions of concentration of the ions Cu^+ and Cu^{2+} in the surface layer were Gaussian ones as well and characterized by the same half-width Δx, as for $k_{523}(x)$. The authors of [8] have obtained that in diffusion from the powder oxide CuO in the samples made as a rectangular parallelepiped with faces parallel to crystallophysic axes X, Y and Z, the dependencies of concentration of the ions Cu^+ and Cu^{2+} on the depth L differed, had a non-monotonic behavior and were characterized by maxima located at $L \approx 400-500\,\mu$m for Cu^+ and $L \approx 200-300\,\mu$m for Cu^{2+}. They note that their obtained distributions $Cu^+(L)$ and $Cu^{2+}(L)$ differ from those predicted in a simple model of thermal diffusion and think it necessary to perform additional studies of its mechanism in case of Cu and lithium niobate.

The coordinate x distributions for the concentration of the ions $C_{Cu^+}(x)$ and $C_{Cu^{2+}}(x)$ in the diffusion X-cut $LiNbO_3:Cu$ are experimentally studied in detail in the paper [11]. The initial congruent lithium niobate plate had a thickness of $d = 1.33$ mm; the diffusion was from the metal film of the thickness of 600 nm deposited to the plate face $x = 0$ by magnetron sputtering during 9 h at the temperature $T = 1000$°C. After diffusion, the $LiNbO_3:Cu$

plate was cut and optically polished to obtain a cuneiform area with an inclination angle $\gamma = 36^\circ$ to the plane $x = d$. The dependencies of the absorption coefficients on the thickness of the cuneiform area h_w have been measured at the wavelengths of 532 and 808 nm, proportional to the concentrations $C_{Cu^+}(x)$ and $C_{Cu^{2+}}(x)$, respectively, thereby enabling the authors of [11] to approximate them by a sum of the two Gaussian functions. It can be assumed that during diffusion both ion types will have a non-zero concentration along the entire thickness of the $LiNbO_3:Cu$ sample. That is why the distributions $C_{Cu^+}(x)$ and $C_{Cu^{2+}}(x)$ shall be described by additionally supplying them with constant components of the small values $C^0_{Cu^+}$ and $C^0_{Cu^{2+}}$ comparable with the accuracy of the experimental measurements for the absorption coefficients. Using the data of [11], as a result we obtain

$$C_{Cu^+}(x) = C^{m1}_{Cu^+}\exp\left[-\frac{(x-x_1^+)^2}{(\Delta x_1^+)^2}\right] + C^{m2}_{Cu^+}\exp\left[-\frac{(x-x_2^+)^2}{(\Delta x_2^+)^2}\right] + C^0_{Cu^+}, \quad (1)$$

$$C_{Cu^{2+}}(x) = C^{m1}_{Cu^{2+}}\exp\left[-\frac{(x-x_1^{2+})^2}{(\Delta x_1^{2+})^2}\right] + C^{m2}_{Cu^{2+}}\exp\left[-\frac{(x-x_2^{2+})^2}{(\Delta x_2^{2+})^2}\right] + C^0_{Cu^{2+}} \quad (2)$$

with the maximum values $C^{m1}_{Cu^+} = 4.20\cdot 10^{25}\,m^{-3}$, $C^{m2}_{Cu^+} = 8.02\cdot 10^{24}\,m^{-3}$, $C^{m1}_{Cu^{2+}} = 2.26\cdot 10^{26}\,m^{-3}$ and $C^{m2}_{Cu^{2+}} = 1.64\cdot 10^{26}\,m^{-3}$ and the space parameters $x_1^+ = 95\,\mu m$, $x_2^+ = 1215\,\mu m$, $\Delta x_1^+ = 310\,\mu m$, $\Delta x_2^+ = 70\,\mu m$, $x_1^{2+} = 225\,\mu m$, $x_2^{2+} = 1245\,\mu m$, $\Delta x_1^{2+} = 130\,\mu m$ and $\Delta x_2^{2+} = 37\,\mu m$. The below-described studies have been performed to evaluate the constant components of the concentrations as $C^0_{Cu^+} = 0.9\cdot 10^{24}\,m^{-3}$ and $C^0_{Cu^{2+}} = 2.0\cdot 10^{25}\,m^{-3}$. Formation of the volume transmission holograms in such samples $LiNbO_3:Cu$ shall be analyzed by taking into account a complex character of distribution of copper ions, which ensure processes of photoexcitation of electrons from the donor centers Cu^+ to the conduction band with their subsequent recombination to the traps Cu^{2+}.

The present paper is dedicated to studying specific features of formation of the photorefractive gratings by means of a fringe pattern of recording laser beams with high contrast in the X-cut $LiNbO_3:Cu$ with different distributions of the ions Cu^+ and Cu^{2+}, with each one of them described by the sum of the constant component and the two Gaussian functions.

Theoretical model and approximations

Let us consider formation of the field of the spatial charge $\mathbf{E}(x,z,t)$ of the photorefractive gratings in approximation of the given light intensity $J(x,z)$ in the interference pattern created by two recording light waves, which symmetrically propagate in relation to the axis X in the $LiNbO_3:Cu$ crystal that is open along the axis Z. We will believe that the quanta of recording radiation of the energy of $\hbar\omega_w$ result in excitation of electrons from the donor centers Cu^+ to the conduction band. This process will be accompanied by optical absorption with an coefficient determined by the following expression [13]:

$$\alpha_w(x) = \hbar\omega_w S_w\left[N_D(x) - N_A(x)\right] = \hbar\omega_w S_w C_{Cu^+}(x), \quad (3)$$

where S_w — a section of photoionization for the centers of this type. As in [12], it is assumed here that the total concentration of the defect centers $N_D(x)$ with photoinduced charge redistribution under heterogeneous illumination and the concentration of the compensating acceptors $N_A(x)$ (in the dark conditions, it is equal to the concentration of ionized donor centers acting as electron traps) are defined by the expressions

$$N_D(x) = C_{Cu^+}(x) + C_{Cu^{2+}}(x) \quad (4)$$

and

$$N_A(x) = C_{Cu^{2+}}(x). \quad (5)$$

Taking into account the dependency of the absorption coefficient on the coordinate x, as determined by the formulas (3) and (1), the distribution of light intensity for the interference pattern in the $LiNbO_3:Cu$ plate can be obtained as follows:

$$J(x,z) = J_0\exp\left\{-\hbar\omega_w S_w\left[\frac{\sqrt{\pi}}{2}\left(C^{m1}_{Cu^+}\Delta x_1^+\left\{\mathrm{erf}\left(\frac{x_1^+}{\Delta x_1^+}\right) + \mathrm{erf}\left(\frac{x-x_1^+}{\Delta x_1^+}\right)\right\} + C^{m2}_{Cu^+}\Delta x_2^+\left\{\mathrm{erf}\left(\frac{x_2^+}{\Delta x_2^+}\right) + \mathrm{erf}\left(\frac{x-x_2^+}{\Delta x_2^+}\right)\right\}\right) + C^0_{Cu^+}x\right]\right\}\left[1 + m\cos\left(\frac{2\pi}{\Lambda}z\right)\right], \quad (6)$$

where $\mathrm{erf}(x/\Delta x)$ — the probability integral [14]. Following the paper [12] and the known single-level model of band transfer [13], we neglect the diffusion mechanism of spatial charge redistribution and the trap saturation effect, and we also use slow varying approximations for all the considered functions along the coordinate x ($\partial J/\partial x \ll \partial J/\partial z$, $|\partial \mathbf{E}/\partial x| \ll |\partial \mathbf{E}/\partial z|$, etc.), the low light intensity $J(x,z)$ and adiabatic tracking of the electron concentration in the conduction band to its time changes. As a result, the equation describing the time evolution of a predominant component of electric field strength for spatial charge $E_z(x,z,t) = E(x,z,t)$ is as follows [12]:

$$\frac{\partial E}{\partial t} + \frac{e\mu S_w}{\varepsilon_3\gamma N_A}(N_D - N_A)JE + \frac{GS_w\hbar\omega_w}{\varepsilon_3}(N_D - N_A)J = 0, \quad (7)$$

where e — the elementary electric charge; ε_3 — the static dielectric permittivity for the field along the polar axis Z;

μ — the mobility of electrons along this axis; G — the Glass constant depending on light polarization forming the photoreactive grating [15]; and γ — the coefficient of two-particle recombination.

For the initial condition $E(x, z, 0) = 0$, which corresponds to switching on the recording light beams at $t = 0$, the solution (7) was obtained in [12] as follows:

$$E(x,z,t) = -\frac{G\hbar\omega_w\gamma N_A(x)}{e\mu}\left\{1 - \exp\left[-\frac{t}{\tau(x)}\right] \times \exp\left[-\frac{mt}{\tau(x)}\cos\left(\frac{2\pi}{\Lambda}z\right)\right]\right\}, \quad (8)$$

where Λ — the spatial period of the grating. However, the relaxation time $\tau(x)$ of this expression will be defined by the complex dependencies (1) and (2) on the coordinate x for the ion concentrations Cu^+ and Cu^{2+}, as well as by distribution of average intensity of light in the crystal, which follows from (6):

$$\frac{1}{\tau(x)} = J_0\frac{e\mu S_w}{\varepsilon_3\gamma}\frac{\begin{array}{c}C^{m1}_{Cu^+}\exp\left[-(x-x_1^+)^2/(\Delta x_1^+)^2\right] \\ +C^{m2}_{Cu^+}\exp\left[-(x-x_2^+)^2/(\Delta x_2^+)^2\right]+C^0_{Cu^+}\end{array}}{\begin{array}{c}C^{m1}_{Cu^{2+}}\exp\left[-(x-x_1^{2+})^2/(\Delta x_1^{2+})^2\right] \\ +C^{m2}_{Cu^{2+}}\exp\left[-(x-x_2^{2+})^2/(\Delta x_2^{2+})^2\right]+C^0_{Cu^{2+}}\end{array}} \times \exp\left\{-\hbar\omega_w S_w\left[\frac{\sqrt{\pi}}{2}\left(C^{m1}_{Cu^+}\Delta x_1^+\left\{\mathrm{erf}\left(\frac{x_1^+}{\Delta x_1^+}\right) + \mathrm{erf}\left(\frac{x-x_1^+}{\Delta x_1^+}\right)\right\} + C^{m2}_{Cu^+}\Delta x_2^+\left\{\mathrm{erf}\left(\frac{x_2^+}{\Delta x_2^+}\right) + \mathrm{erf}\left(\frac{x-x_2^+}{\Delta x_2^+}\right)\right\}\right) + C^0_{Cu^+}x\right]\right\}. \quad (9)$$

As noted in [12], the photorefractive grating's spatial charge field forming in the $LiNbO_3:Cu$ plate is a superposition of spatial harmonics of this kind

$$E_{sc}^{(n)}(x,z,t) = E_n(x,t)\cos(2\pi n/\Lambda) \quad (10)$$

with the numbers $n = 0, 1, 2, \ldots$ and the amplitudes $E_n(x,t)$. These amplitudes can be found using decomposition of the last exponential multiplier of (8) into a series by the modified Bessel functions of the nth order, $I_n\big(mt/\tau(x)\big)$. For the amplitude of the first harmonic $E_n(x,t)$ at $n = 1$ of (10), which defines the efficiency of Bragg diffraction on the photorefractive grating, the following analytical expression can be found from the relationships (8), (5) and (2):

$$E_1(x,t) = -\frac{2G\hbar\omega_w\gamma}{e\mu}\left\{C^{m1}_{Cu^{2+}}\exp\left[-\frac{(x-x_1^{2+})^2}{(\Delta x_1^{2+})^2}\right] + C^{m2}_{Cu^{2+}} \times \exp\left[-\frac{(x-x_2^{2+})^2}{(\Delta x_2^{2+})^2}\right] + C^0_{Cu^+}\right\}I_1\left(\frac{mt}{\tau(x)}\right)\exp\left(-\frac{t}{\tau(x)}\right). \quad (11)$$

As follows from (11), in the considered $LiNbO_3:Cu$ sample the dynamics of formation of the photorefractive hologram (for which the efficiency of Bragg diffraction of a probing beam is exactly defined by the field amplitude of the first spatial harmonic) has a complex character depending on distributions for the concentrations of copper ions in both the charge states $C_{Cu^+}(x)$ and $C_{Cu^{2+}}(x)$. However, at the initial section, at $t \ll \tau(x)$ this amplitude rises in time by the linear law, as follows from (11) and (9). At the same time, the heterogeneous spatial distribution along the coordinate x remains at this section and is determined only by distribution of the photovoltaically active donor centers $C_{Cu^+}(x)$:

$$E_1^{in}(x,t) = -mJ_0\frac{G\hbar\omega_w S_w}{\varepsilon_3}t\left\{C^{m1}_{Cu^+}\exp\left[-\frac{(x-x_1^+)^2}{(\Delta x_1^+)^2}\right] + C^{m2}_{Cu^+}\exp\left[-\frac{(x-x_2^+)^2}{(\Delta x_2^+)^2}\right] + C^0_{Cu^+}\right\}\exp\left\{-\hbar\omega_w S_w \times \left[\frac{\sqrt{\pi}}{2}\left(C^{m1}_{Cu^+}\Delta x_1^+\left\{\mathrm{erf}\left(\frac{x_1^+}{\Delta x_1^+}\right) + \mathrm{erf}\left(\frac{x-x_1^+}{\Delta x_1^+}\right)\right\} + C^{m2}_{Cu^+}\Delta x_2^+\left\{\mathrm{erf}\left(\frac{x_2^+}{\Delta x_2^+}\right) + \mathrm{erf}\left(\frac{x-x_2^+}{\Delta x_2^+}\right)\right\}\right) + C^0_{Cu^+}x\right]\right\}. \quad (12)$$

Reasonably, the diffraction efficiency of the considered photorefractive hologram shall be monitored using laser radiation of the wavelength of $\lambda_r > \lambda_w$, at which the $LiNbO_3:Cu$ sample has low photorefractive sensitivity and a negligible average absorption coefficient [10,12]. In this case, the efficiency of Bragg diffraction to the first order will be the greatest at an unusual probing beam of the value $\eta(t)$, which is defined by the amplitude of perturbation of the unusual refraction index as created by the recording beams in the $LiNbO_3:Cu$ plate:

$$\Delta n_e(x,t) = -\frac{n_e^3 r_{33}}{2}E_1(x,t), \quad (13)$$

where n_e — the unusual refraction index of the undisturbed crystal and r_{33} — its electro-optical constant. For the small values of $\eta(t)$, which do not exceed several percent, theoretical analysis can neglect the change of the amplitude of a reading wave A_r by transforming into a diffracted beam. By neglecting its optical absorption as well, taking into account the smallness of the Bragg angle θ_B of the probing beam's incident beam θ_i and using the known approach [16,17], the equation of spatial evolution of the amplitude of the diffracted light wave $A_d(x,t)$ taking into account (13) is presented as follows:

$$\frac{dA_d}{dx} = -i\frac{\pi}{2\lambda_r}n_e^3 r_{33}E_1(x,t)A_r\exp(i\Delta kx) \quad (14)$$

with a parameter of wave detuning, which is defined be crystal deviation of the probing beam incident angle

θ_i from θ_B:

$$\Delta k \simeq \frac{2\pi}{\Lambda}(\sin\theta_i - \sin\theta_B). \qquad (15)$$

The relationships obtained within the framework of the considered model make it possible to describe formation of the spatial charge field and the time dynamics of diffraction efficiency of the photorefractive holograms formed in the *X*-cut $LiNbO_3:Cus$ with different distributions of the ions Cu^+ and Cu^{2+}, with each of them described by the sum of the constant component and the two Gaussian functions, by means of the interference pattern of the recording laser beams with high contrast.

Experiment

The dynamic photorefractive holograms with the spatial period of $\Lambda = 12\,\mu$m have been formed using the interference pattern with the contrast $m \approx 0.98$ and the lattice vector parallel to the polar axis *Z* for the two recording laser beams with the wave length of $\lambda_w = 532$ nm and the powers $P_1 \approx 0.98$ mW, $P_2 \approx 1.45$ mW. They corresponded to the usual waves, had an aperture $D_w = 1.1$ mm and provided the average intensity of the interference pattern $J_0 \approx 472\,\text{W/m}^2$ at an input face $x = 0$ (see the formula (6)) of the above-described $LiNbO_3:Cu$ sample with the distributions of the concentration of copper ions approximated by the relationships (1) and (2). In the same way as in [12], the diffraction efficiency of the formed volume grating has been monitored by the probing beams of the semiconductor laser with $\lambda_r = 650$ nm and the power of 4.3 mW, which propagates in the form of the unusual wave at the respective Bragg angle to the axis *X* of the sample. The dependency of rise of the diffraction efficiency $\eta_{in}(t)$ at the initial section of recording of the photorefractive grating (measured using the photodiode PD-24K and the digital oscilloscope Tektronix TDS2022C) as dotted on Fig. 1 has been satisfactorily approximated by the function

$$\eta_{in}(t) = bt^2 + ct^3, \qquad (16)$$

shown by the solid curve, with the values of the coefficients $b = 7.63 \cdot 10^{-5}\,\text{s}^{-2}$ and $c = -2.66 \cdot 10^{-6}\,\text{s}^{-3}$.

The angular selectivity has been experimentally studied at the wavelength $\lambda_r = 650$ nm for the photorefractive hologram with the same spatial period $\Lambda = 12\,\mu$m and wit the diffraction efficiency approaching $\eta_m = 0.003$ provided that the Bragg condition is exactly met. Its recording time at $\lambda_w = 532$ nm and the beam powers $P_1 \approx 0.95$ mW and $P_2 \approx 1.46$ mW ($m \approx 0.98$) was 7 s. After hologram formation, the $LiNbO_3:Cu$ sample was placed on a rotary table designed to fix an offset $\Delta\theta = \theta_{ia} - \theta_{Ba}$ of the air light incident angle θ_{ia} to the input face $x = 0$ from the air Bragg angle θ_{Ba} with and accuracy of up to one angular minute. The dependency of the diffracted light power on the offset angle was registered for $\Delta\theta \geq 0$ under the assumption of its symmetry. Fig. 2 shows the normalized experimental angular dependency of the diffraction efficiency $\eta(\Delta\theta)$ (shown by the circles) measured using the power measuring device PM130D and its assumed behavior for $\Delta\theta < 0$ shown by the triangle.

The solid curve of this figure shows the known Kogelnik's theoretical dependency [16] for the angular selectivity of the volume sinusoidal phase grating with homogeneous distribution of perturbations of the refraction index $\Delta n_m(x)$, as calculated at $0 \leq x \leq d_{ef}$ for the effective interaction length $d_{ef} = 0.7$ mm. In this approximation, without taking into account real distribution $\Delta n_m(x)$ across the studied sample, this dependency satisfactorily describes only the basic maximum of the selectivity curve.

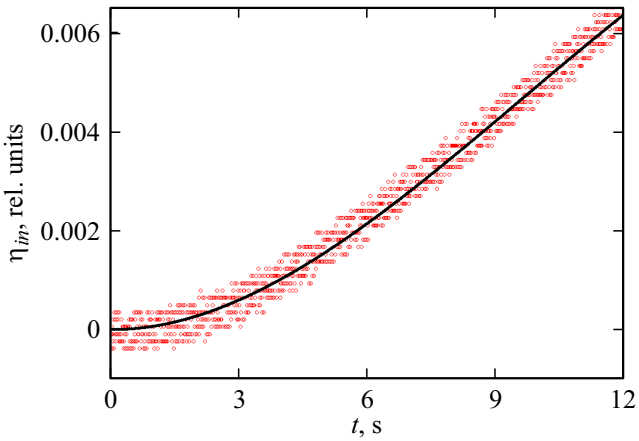

Figure 1. Time dependency of the diffraction efficiency at the initial section of formation of the dynamic photorefractive grating in the studied $LiNbO_3:Cu$ sample. Dots — experimental data; solid line — approximation by the formula (16) at $b = 7.63 \cdot 10^{-5}\,\text{s}^{-2}$ and $c = -2.66 \cdot 10^{-6}\,\text{s}^{-3}$.

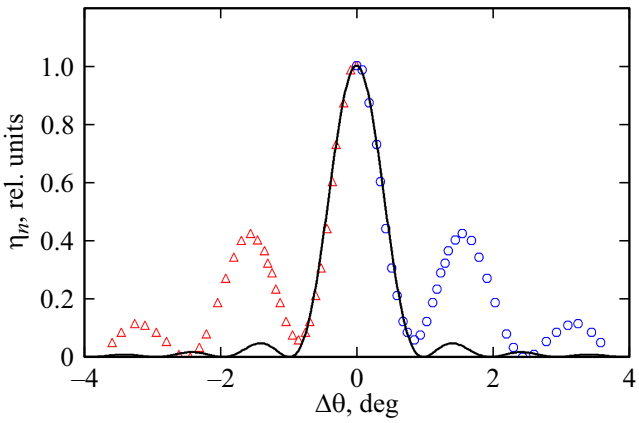

Figure 2. Dependency of the normalized diffraction efficiency on the offset angle $\Delta\theta = \theta_{ia} - \theta_{Ba}$ between the air incident angle and the air Bragg angle. The circles — experimental data, the triangles — reflection of the experimental data onto the region $\Delta\theta < 0$, the solid curve — calculation as per the Kogelnik formula.

Evaluation of the Glass constant and analysis of angular selectivity

The quadratic time dependency of Fig. 1 for the diffraction efficiency $\eta_{in}(t)$ at the initial section of formation of the photorefractive hologram by the usual light beams with $\lambda_w = 532\,\text{nm}$ will be described by us following the approach of [12], using the relationship (12) for $E_1^{in}(x,t)$ at the respective Glass constant G_0. The subsequent substitution of $E_1^{in}(x,t)$ into (14) and its integration provided that the Bragg condition is exactly met $\Delta k = 0$, makes it possible to present the dependency $\eta_{in}(t)$ as follows:

$$\eta_{in}(t) = \left(\frac{\pi n_e^3 r_{33}}{2\lambda_r} \frac{G_0 \hbar \omega_w S_w C_{Cu^+}^{m1} m J_0}{\varepsilon_3} d_{\text{ef}}^{in} \right)^2 t^2, \qquad (17)$$

where the effective interaction length is defined by the integral expression

$$d_{\text{ef}}^{in} = \int_0^d \left\{ \exp\left[-\frac{(x - x_1^+)^2}{(\Delta x_1^+)^2} \right] + \frac{C_{Cu^+}^{m2}}{C_{Cu^+}^{m1}} \exp\left[-\frac{(x - x_2^+)^2}{(\Delta x_2^+)^2} \right] + \frac{C_{Cu^+}^{0}}{C_{Cu^+}^{m1}} \right\} \exp\left\{ -\hbar \omega_w S_w \left[\frac{\sqrt{\pi}}{2} \left(C_{Cu^+}^{m1} \Delta x_1^+ \left\{ \text{erf}\left(\frac{x_1^+}{\Delta x_1^+} \right) + \text{erf}\left(\frac{x - x_1^+}{\Delta x_1^+} \right) \right\} + C_{Cu^+}^{m2} \Delta x_2^+ \left\{ \text{erf}\left(\frac{x_2^+}{\Delta x_2^+} \right) + \text{erf}\left(\frac{x - x_2^+}{\Delta x_2^+} \right) \right\} \right) + C_{Cu^+}^{0} x \right] \right\} dx. \qquad (18)$$

Comparing the equations (16) and (17) with taking into account (18), and using the above-said parameters of the diffusion $LiNbO_3:Cu$ structure, the conditions and results of the experiment, the photoionization section $S_w = 2.0 \cdot 10^{-4}\,\text{m}^2/\text{J}$ [12], the literature data for the constitutive parameters of [15,18], and the values $C_{Cu^+}^0 = 9 \cdot 10^{23}\,\text{m}^{-3}$ made it possible to evaluate the effective interaction length at the initial section of formation of the photorefractive hologram as $d_{\text{ef}}^{in} \approx 0.23\,\text{mm}$ and the Glass constant for the recording usual waves with $\lambda_w = 532\,\text{nm}$ as $G_0 \approx 8.0\,\text{pm/V}$. In terms of the magnitude order, the obtained value is close in terms of the magnitude order to the Glass constant of [15] for the $LiNbO_3:Cu$ crystals with volume doping, which is 5.5 pm/V.

With small values and arbitrary time of formation in the considered diffusion $LiNbO_3:Cu$ structure, the normalized angular dependency of the diffraction efficiency of the photorefractive hologram can be obtained from (14) and (15)

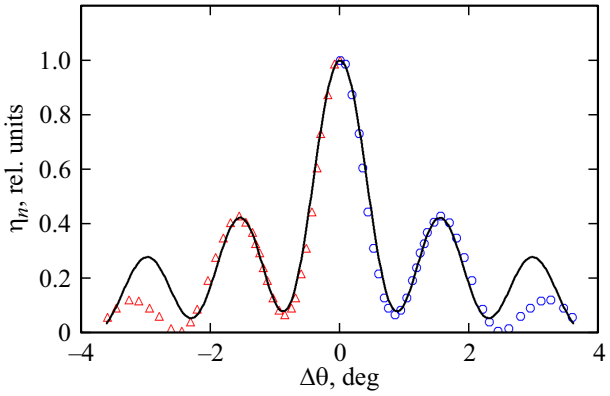

Figure 3. Dependency of the normalized diffraction efficiency on the offset angle $\Delta\theta$ between the incident angle θ_{ia} and the air Bragg angle θ_{Ba}, $\Delta\theta = \theta_{ia} - \theta_{Ba}$. The dots correspond to the data of Fig. 2. The solid curve — the calculated dependency as per the relationships (19), (11) and (9).

as follows:

$$\eta_n(\theta_{ia}, t) = \left| \int_0^d E_1(x,t) \exp\left[i \frac{2\pi}{\Lambda n_e} \left(\sin\theta_{ia} - \frac{\lambda_r}{2\Lambda} \right) \right] dx \right|^2 \Big/ \left| \int_0^d E_1(x,t) dx \right|^2, \qquad (19)$$

where the amplitude of the first spatial harmonic $E_1(x,t)$ is determined by the relationships (11) and (9). The results of numerical simulation of this angular dependency for the values of the used fitting parameters $C_{Cu^+}^0 = 9 \cdot 10^{23}\,\text{m}^{-3}$, $C_{Cu^{2+}}^0 = 2 \cdot 10^{25}\,\text{m}^{-3}$ and $\gamma/\mu = 5.7 \cdot 10^{-12}\,\text{m} \cdot \text{V}$ are shown on Fig. 3 by the solid curve. As follows from Fig. 3, the curve of the angular selectivity is satisfactorily described for its three main petals by the used model of formation of the spatial charge field of the photorefractive hologram using the interference pattern with high contrast $m \approx 1$ in the studied diffusion X-cut $LiNbO_3:Cu$ crystal, whereas the model assumes that it has different distributions of the ions Cu^+ and Cu^{2+}, with each of them is the sum of the constant component and the two Gaussian functions. The significant differences between the experimental and calculated data for the setoff from the Bragg angle $|\Delta\theta| > 2.2\,\text{deg}$ can be related to accepted approximations and errors in determination of the parameters for the distributions $C_{Cu^+}(x)$ and $C_{Cu^{2+}}(x)$.

Numerical simulation of spatial distribution and dynamics of the field of spatial charge

At various times after starting to record the photorefractive hologram, the distribution of the amplitude of the spatial charge field $E_1(x,t)$ along the crystal depth can

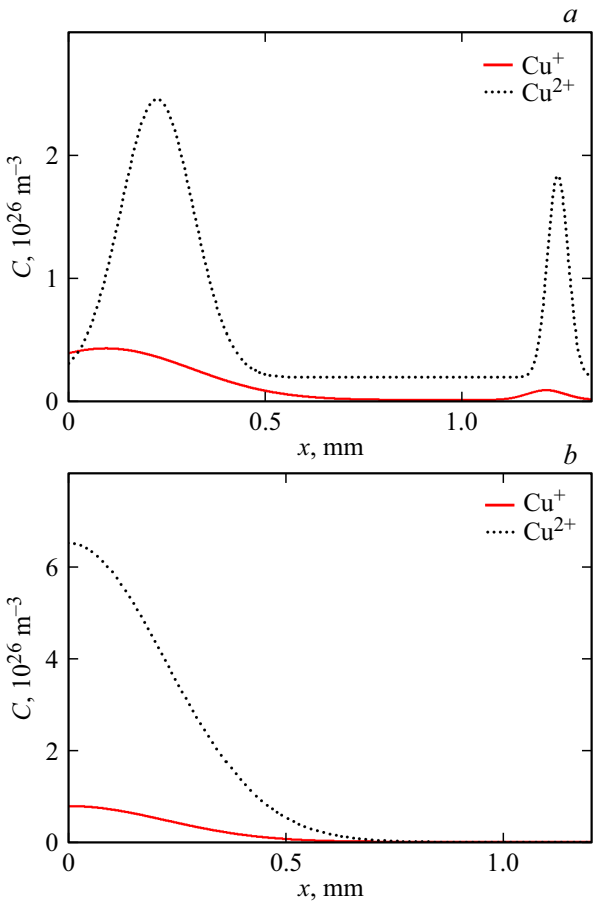

Figure 4. Distributions of the ion concentrations in the charge states Cu^+ and Cu^{2+} along the diffusion $LiNbO_3:Cu$ samples described in the present paper (*a*) and in [12] (*b*).

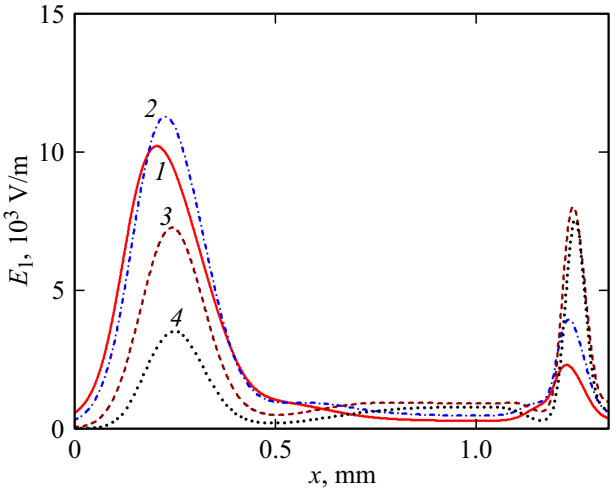

Figure 5. Distribution of the amplitude of the first spatial harmonic field of the photorefractive hologram with the spatial period of $12\,\mu$m along the depth inside the diffusion X-cut $LiNbO_3:Cu$ sample described in the present paper, with the dependencies $C_{Cu^+}(x)$ and $C_{Cu^{2+}}(x)$ shown on Fig. 4, *a*, when recording the interference pattern with the intensity $J_0 \approx 472\,W/m^2$ and the contrast $m \approx 0.98$ at the various times $t_w = 1$ (*1*), 2 (*2*), 8 (*3*) and 24 s (*4*).

be calculated using the relationships (11) and (9). As follow from them, the amplitude $E_1(x,t)$ in a complicated way depends on the distributions of the ion concentrations $C_{Cu^+}(x)$ and $C_{Cu^{2+}}(x)$ across the crystal. Below, we limit ourselves to analysis of the two $LiNbO_3:Cu$ structures, while the first of them is discussed above, and the second one is described in the paper [12], with the distributions of the concentrations of copper ions shown on Fig. 4, *a* and Fig. 4, *b*, respectively.

It should be noted that in the first $LiNbO_3:Cu$ sample there is different localization of the main maxima for the distributions of the donor and trap centers that are presented by the ions in the charge states Cu^+ and Cu^{2+}, respectively. At the same time, the trap concentrations near the crystal faces $x = 0$ and $x = d = 1.33$ mm have a significantly smaller value than at a distance from them, $x = 225\,\mu$m and $x = 1245\,\mu$m.

Fig. 5 shows the results of calculation of $E_1(x,t_i)$ for this $LiNbO_3:Cu$ sample at the above-discussed parameters of the distributions $C_{Cu^+}(x)$ and $C_{Cu^{2+}}(x)$ and the experimentally obtained evaluations for G_0 and γ/μ, using the value of the photoionization section $S_w = 2.0 \cdot 10^{-4}\,m^2/J$ [12] and the literature data for the constitutive parameters of niobate lithium from [15,18].

As it is clear from Fig. 5, the studied $LiNbO_3:Cu$ structure has a complex nature of the dynamics of formation of the first spatial harmonic of the electric field of the hologram with the amplitude $E_1(x,t)$ Already at the initial stage of recording, at $t_w = 1$ s (the curve *2*) the coordinate dependency of the filed amplitude does not correspond to the distribution of the concentration of the donor centers $C_{Cu^+}(x)$ along the crystal depth (Fig. 4, *a*). The calculations have shown that for the used parameters of the model and the experiment conditions, the duration of the initial section (when the dynamics of the spatial charge field is mainly contributed by the process of electron photoexcitation to the conduction band from the donor centers Cu^+ and it can be described by the relationship (12)), does not exceed 0.01 s. After that, the major role is played by the conduction current, whose value is proportional to the mobility of electrons μ, and their recombination from the conduction band to the trap centers Cu^{2+} at the rate defined the by value $\left(\gamma C_{Cu^{2+}}(x)\right)^{-1}$. The value $\gamma/\mu = 5.7 \cdot 10^{-12}\,m \cdot V$ (used in numerical simulation of the dynamics of the field amplitude $E_1(x,t)$), which is found from fitting the curve of angular selectivity (Fig. 3), is substantially different from the literature data for the volume-doped $LiNbO_3:Cu$ crystals, $\gamma/\mu = 7.2 \cdot 10^{-9}\,m \cdot V$ (see, for example, [12]). Further research is required for the reasons for such a difference for the studied structure with diffusion doping.

It is typical that the amplitude of the first spatial harmonic of the electric field of the photorefractive hologram at the boundary $x = 0$ of this structure $E_1(0,t)$ decrease

with a recording time. That is why it is unsuitable for implementation of the photovoltaic tweezers based thereon. It follows from Fig. 4, *a* and Fig. 5 that the maxima of this amplitude approximately correspond to the maxima in the distribution of the trap concentration $C_{Cu^{2+}}(x)$.

Fig. 6 shows the results of calculation $E_1(x, t_w)$ for the $LiNbO_3:Cu$ structure described in the paper [12], using the values thereof for the constitutive parameters $G_e \approx 4.6$ pm/V, $\gamma = 5.3 \cdot 10^{-13}$ m^3/s, $\mu = 7.4 \cdot 10^{-5}$ m^2/V $\cdot$ s and for the Gaussian distributions of concentration of copper ions $C^m_{Cu^+} = 7.8 \cdot 10^{24}$ m^{-3}, $C^m_{Cu^{2+}} = 6.5 \cdot 10^{25}$ m^{-3} and $\Delta x^+ = \Delta x^{2+} = 316\,\mu$m, as well as for the experimental characteristics of the recording interference pattern $m = 1$ and $J_0 = 2600$ W/m^2.

With a coinciding nature of the distributions of the donor and trap centers, such a sample exhibits monotonic time increase of the amplitude of the first spatial harmonic $E_1(x, t_w)$ along its entire depth. At the same time, its maximum value falls to the $LiNbO_3:Cu$ structure boundary $x = 0$, thereby providing, when $x < 0$, significant evanescent field with the amplitudes above 1 MV/m at the recording times $t_w > 60$ s. Thus, the photovoltaic tweezers are implemented in an optimum way by using the diffusion X-cut $LiNbO_3:Cu$ samples with close distributions of the donor (Cu^+) and trap (Cu^{2+}) centers, with the maxima localized near the boundary designed to capture micro- and nano-objects by dielectrophoretic forces. Creation of these structures requires a correct model of processes of diffusion of copper into the lithium niobate crystals, which is not available now.

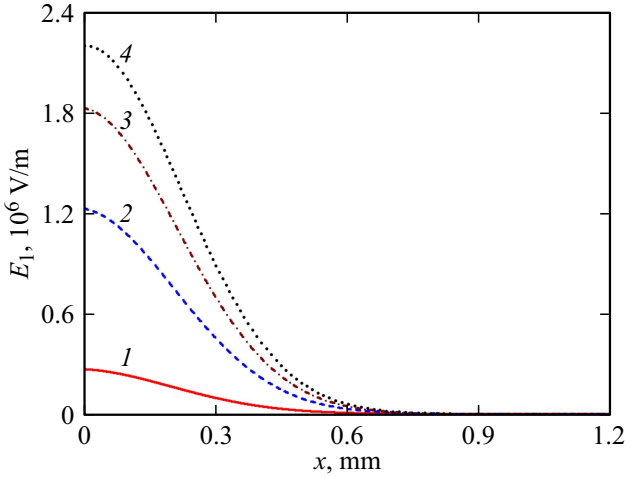

Figure 6. Distribution of the amplitude of the first spatial harmonic of the photorefractive hologram with the spatial period of 2.5 μm along the depth for the diffusion X-cut $LiNbO_3:Cu$ sample described in [12], with the dependencies $C_{Cu^+}(x)$ and $C_{Cu^{2+}}(x)$ shown on Fig. 4, *b*, when recording the fringe pattern with the intensity $J_0 = 2600$ W/m^2 and the contrast $m = 1$ during the different intervals of time: $t_w = 10$ (*1*), 60 (*2*), 120 (*3*) and 270 s (*4*).

Conclusion

Thus, the paper has dealt with the specific features of formation of the volume transmission holograms in the X-cut lithium niobate plates with diffusion doping by copper in order to implement the photovoltaic tweezers. The experimental studies and the numerical simulation have been performed for the X-cut $LiNbO_3:Cu$ sample described in [9], which had suggested to approximate the distribution of the concentration of copper ions in the charge states Cu^+ and Cu^{2+} by the different sums of the two Gaussian functions. In assuming that during diffusion both ion types can have a non-zero concentration along the entire thickness of the $LiNbO_3:Cu$ plate, in the numerical simulation also included the constant components of the concentrations with the small values $C^0_{Cu^+}$ and $C^0_{Cu^{2+}}$ into these distributions. The approach developed in [12] has been used to obtain (in the approximations of the given light intensity in the interference pattern with arbitrary contrast, no saturation of the traps and the diffusion current, and of slow varying of all the functions along the coordinate x) the analytical expressions for description of time evolution of the amplitude of the first spatial harmonic of the field $E_1(x, t)$, which take into account heterogeneities of the ion distributions Cu^+ and Cu^{2+} and the absorption index of the recording beams along the sample thickness.

Comparing the results of the experimental studies of the Bragg diffraction efficiency of the reading beam for the initial section of formation of the photorefractive hologram ($t_w < 3$ s) and its angular selectivity (with the recording time $t_w = 7$ s, for the fringe pattern of the recording light beams ($\lambda_w = 532$ nm) with the contrast $m \approx 0.98$ and the average intensity $J_0 \approx 470$ W/m^2) with the obtained theoretical relationships has evaluated the constitutive parameters of the $LiNbO_3:Cu$ structure. These parameters include the Glass constant for the usual waves $G_0 \approx 8.0$ pm/V, the ration of the coefficient of two-particle recombination to the mobility of electrons along the polar axis $\gamma/\mu = 5.7 \cdot 10^{-12}$ m $\cdot$ V and the constant components in the distributions of the concentrations of copper ions $C^0_{Cu^+} = 9 \cdot 10^{23}$ m^{-3} and $C^0_{Cu^{2+}} = 2 \cdot 10^{25}$ m^{-3}.

Using the numerical simulation, the obtained relationships have been subjected to comparative analysis of the spatial distribution for the amplitude of the first harmonic of the electric field of the photorefractive hologram in the two $LiNbO_3:Cu$ structures: one considered in the present paper and one described in [12]. It has been established that the amplitude of the first spatial harmonic of the electric field of photorefractive hologram for the first structure had its maximum, which approximately corresponded to the maximum in the distribution of the trap concentration $C^0_{Cu^{2+}}(x)$ at the distance of about 250 μm from the boundary $x = 0$, where the field $E_1(0, t)$ is small and decreases with the recording time. That is why these structures are unsuitable for implementation of the photovoltaic tweezer based thereon. The second structure (with the Gaussian

distributions of concentration of the donor and trap centers, with localization of the maxima $C^m_{Cu^+}$ and $C^m_{Cu^{2+}}$, respectively at $x = 0$) exhibits the monotonic time increase in the amplitude of the first spatial harmonic $E_1(x, t)$ along its entire depth, with the maximum value $E_1(0, t)$. At the recording time of the hologram $t_w > 60$ s, this structure realizes the evanescent fields with the amplitudes above 1 MV/m. It can be concluded that the tweezers shall be implemented by using the diffusion X-cut $LiNbO_3 : Cu$ structures with close distributions of the donor (Cu^+) and trap (Cu^{2+}) centers, with the maxima localized near the boundary designed to capture micro- and nano-particles by dielectrophoretic forces.

Funding

The paper was supported by the Ministry of Science and Higher Education of the Russian Federation within the framework of the State Assignment FEWM-2023-0012 for 2023.

Conflict of interest

The authors declare that they have no conflict of interest.

References

[1] J. Villarroel, H. Burgos, Á. García-Cabañes, M. Carrascosa, A. Blázquez-Castro, F. Agulló-López. Opt. Express, **19** (24), 24320 (2011). DOI: 10.1364/OE.19.024320
[2] M. Esseling, A. Zaltron, N. Argiolas, G. Nava, J. Imbrock, I. Cristiani, C. Sada, C. Denz. Appl. Phys. B, **113** (2), 191 (2013). DOI: 10.1007/s00340-013-5456-8
[3] J. Matarrubia, A. García-Cabañes, J.L. Plaza, F. Agulló-López, M. Carrascosa. J. Phys. D: Appl. Phys., **47** (26), 265101 (2014). DOI: 10.1088/0022-3727/47/26/265101
[4] M. Carrascosa, A. García-Cabañes, M. Jubera, J.B. Ramiro, F. Agulló-López. Appl. Phys. Rev., **2** (4), 040605 (2015). DOI: 10.1063/1.4929374
[5] A. Blázquez-Castro, A. García-Cabañes, M. Carrascosa. Appl. Phys. Rev., **5** (4), 41101 (2018). DOI: 10.1063/1.5044472
[6] K.M. Mambetova, S.M. Shandarov, A.I. Tatiannikov, S.V. Smirnov. Izv. vuzov. Fizika, **62** (4), 89 (2019) (in Russian). DOI: 10.17223/00213411/62/4/89
[7] S. Kar, K.S. Bartwal. Materials Lett., **62** (24), 3934 (2008). DOI: 10.1016/j.matlet.2008.05.031
[8] D. Sugak, I.I. Syvorotka, U. Yakhnevych, O. Buryy, N. Martynyuk, S. Ubizskii, Ya. Zhydachevskyy, A. Suchocki, H. Kumar, V. Janyani, G. Singh. Acta Physica Polonica A, **133** (4), 965 (2018). DOI: 10.12693/APhysPolA.133.965
[9] K. Peithmann, J. Hukriede, K. Buse, E. Krätzig. Phys. Rev. B, **61** (7), 4615 (2000). DOI: 10.1103/PhysRevB.61.4615
[10] K.M. Mambetova, N.N. Smal', S.M. Shandarov, L.N. Orlikov, S.I. Arestov, S.V. Smirnov. Izv. vuzov. Radiofizika, **57** (8), 675 (2014) (in Russian).
[11] A.A. Kolmakov, A.S. Temereva, R.I. Anisimov, A.V. Mikhailenko, S.M. Shandarov, I.V. Timofeev, M.V. Pyatnov. V sb.: *Sbornik trudov XXXIII Vserossiiskoi shkoly-seminara „Volnovye yavleniya: fizika i primeneniya" im. A.P. Sukhorukova („Volny-2022")*, pod red. A.N. Kalisha (M., 2022), s. 58 (in Russian).
[12] K.M. Mambetova, S.M. Shandarov, L.N. Orlikov, S.I. Arestov, S.V. Smirnov, L.Ya. Serebrennikov, V.A. Krakovskii. Opt. i spektr., **126** (6), 23 (2019) (in Russian). DOI: 10.21883/OS.2019.06.47782.31-19
[13] S.M. Shandarov, V.M. Shandarov, A.E. Mandel, N.I. Burimov. *Fotoreaktivnye effekty v elektrooptic heskikh kristallakh: monografiya* (Tomsk: Tomsk. gos. un-t sistem upr. i radioelektroniki, 2012) (in Russian).
[14] A. Ango. *Matematika dlya elektro- i radioinzhenerov* (M.: Nauka, 1967) (in Russian).
[15] T. Volk, M. Wöhlecke. *Lithium Niobate: Defects, Photorefraction and Ferroelectric Switching,* 1st ed. (Springer Berlin, Heidelberg, 2008). DOI: 10.1007/978-3-540-70766-0
[16] H. Kogelnik. Bell. Syst. Techn. J., **48** (9), 2909 (1969). DOI: 10.1002/j.1538-7305.1969.tb01198.x
[17] L.N. Magdich, V.Ya. Molchanov. *Akustoopticheskie ustroistva i ikh primenenie* (Sov. Radio, M., 1978) (in Russian).
[18] M.P. Petrov, S.I. Stepanov, A.V. Knomenko. *Photoreaktivnye kristally v kogerentnoi optike* (Nauka, SPb., 1992) (in Russian).

Translated by M.Shevelev